Spectral fluctuation and $1/f^{\alpha}$ noise in the energy level statistics of interacting trapped bosons

Kamalika Roy,[1] Barnali Chakrabarti,[1,2] Anindya Biswas,[3,4,*] V. K. B. Kota,[5] and Sudip Kumar Haldar[1]

[1]*Department of Physics, Lady Brabourne College, P1/2 Suhrawardi Avenue, Kolkata 700017, India*

[2]*Instituto de Fisica, Universidade de São Paulo, Caixa Postale 66318, 05315-970, São Paulo, SP, Brazil*

[3]*Department of Physics, University of Calcutta, 92 A.P.C. Road, Calcutta 700009, India*

[4]*Harish-Chandra Research Institute, Chhatnag Road, Jhunsi, Allahabad 211019, India*

[5]*Physical Research Laboratory, Navarangpura, Ahmedabad 380009, India*

(Received 3 February 2012; revised manuscript received 3 May 2012; published 20 June 2012)

It has been recently shown numerically that the transition from integrability to chaos in quantum systems and the corresponding spectral fluctuations are characterized by $1/f^{\alpha}$ noise with $1 \leqslant \alpha \leqslant 2$. The system of interacting trapped bosons is inhomogeneous and complex. The presence of an external harmonic trap makes it more interesting as, in the atomic trap, the bosons occupy partly degenerate single-particle states. Earlier theoretical and experimental results show that at zero temperature the low-lying levels are of a collective nature and high-lying excitations are of a single-particle nature. We observe that for few bosons, the $P(s)$ distribution shows the Shnirelman peak, which exhibits a large number of quasidegenerate states. For a large number of bosons the low-lying levels are strongly affected by the interatomic interaction, and the corresponding level fluctuation shows a transition to a Wigner distribution with an increase in particle number. It does not follow Gaussian orthogonal ensemble random matrix predictions. For high-lying levels we observe the uncorrelated Poisson distribution. Thus it may be a very realistic system to prove that $1/f^{\alpha}$ noise is ubiquitous in nature.

DOI: 10.1103/PhysRevE.85.061119 PACS number(s): 05.40.Ca, 05.45.Mt, 03.75.Hh

I. INTRODUCTION

Although there is no precise definition of quantum chaos, it is closely related to the energy level fluctuation properties of a quantum system. Bohigas *et al*. conjectured that the level fluctuation of a quantum system whose classical limit is chaotic is described by the random matrix theory (RMT) [1], whereas spectral fluctuation of a classically integrable system obeys Poisson statistics [2]. The concept of quantum chaos plays an important role in the understanding of the universal properties of the energy level spectrum of quantum systems. However, complex natural systems are neither fully integrable nor fully chaotic, and they attain special interest. The RMT introduced by Wigner has been widely used in the description of the complex spectrum of an atomic nucleus, atoms, and molecules [3–5]. On the other hand, bosonic ensembles in the dense limit may be ergodic with an increase in the number of single-particle states [6]. In last few years, interacting bosonic systems have been of special interest due to the experimental observation of Bose-Einstein condensation [7–10]. The presence of an external harmonic trap makes it more interesting because, as stated by Asaga *et al*., in an atomic trap, bosonic atoms occupy partly degenerate single-particle states [11]. Although it is argued that the random matrix approach should reveal the generic features of the spectrum, there is neither analytical treatment nor systematic numerical calculations in this direction. The chaotic signature in the time evolution of Bose-Einstein condensation (BEC) driven by the time-periodic harmonic or kicked pulses is observed [12–14]. But energy level statistics of the experimentally dilute BEC has not been studied yet. In the earlier analysis by Bohigas *et al*. of nuclear and atomic spectra the nearest-neighbor spacing distribution agrees very well with a Gaussian orthogonal ensemble (GOE) [15]. However, for the interacting trapped bosons, it seems to contradict the usual expectation based on RMT. Very recently, spectral properties of trapped one-dimensional (1D) ultracold fermions in optical lattices have been studied, and the interplay of the repulsive interaction with the external harmonic trap was observed [16]. So it is also very interesting to study the energy level statistics of trapped bosons which are spatially inhomogeneous, and we may expect new and rich physics.

Recently, a different approach to characterize quantum chaos has been proposed based on the idea that the corresponding energy level sequence is analogous to the discrete time series. The level fluctuation is well characterized by the Fourier power spectrum, and a power law behavior has been identified. It is conjectured that spectral fluctuations of chaotic quantum systems are characterized by $1/f$ noise, whereas complete integrable systems exhibit $1/f^2$ noise [17–20]. The earlier studies in this direction involve quantum billiards, nonintegrable coupled quartic oscillators, kicked tops, and integrable spin chains [19,21–23]. In this work we study the system of N interacting bosons at zero temperature in the presence of an external trap. The choice of such a system is important for various reasons. First, it is an inhomogeneous and complex system due to the presence of two energy scales. Interatomic interaction is characterized by Na_s, where a_s is the s-wave scattering length, and the external trap energy is characterized by $\hbar\omega$, where ω is the external trap frequency. From the earlier theoretical and experimental results it is an established fact that at zero temperature the low-lying collective excitations are strongly affected by the interatomic interaction when the high-lying excitations are of a single-particle nature [22,24–26]. The transition from collective to single-particle excitations makes us more curious to study the level fluctuation and to verify whether $1/f^{\alpha}$ noise is ubiquitous in nature. Second, the system directly manifests the experimental Bose-Einstein condensation [7–10]. For the

*Corresponding author: anindyabiswas@hri.res.in

present calculation we consider the N-body bosonic system at zero temperature. There may be a very small effect from the thermal cloud around the condensate even at zero temperature, and the condensate is depleted due to the interaction [27]. However, for the present calculation we ignore that as the whole condensate is described by a single and fixed scattering length and the condensate is extremely dilute. Thus the effect of damping does not appear in our present calculation. However, the effect of damping may be important when the interaction is tuned by the external magnetic field. Thus the system in our present work is neither fully chaotic (for low-lying levels) nor fully integrable (for high-lying levels) due to the interplay of two energy scales. At this point we should mention that Bohigas *et al*. analyzed thoroughly the nuclear shell model and neutron resonance data for different nuclei. The nearest-neighbor spacing distribution of the nuclear data ensemble (NDE) agrees very well with the GOE prediction [15]. In the atomic spectra the levels with the same quantum numbers also show a Wigner type spacing distribution. Thus in nuclear and atomic spectra, the regular features of the low-lying part of the spectrum and the chaotic features of the high-lying collective levels are well established fact. However, for the interacting trapped bosons, it seems to contradict the usual expectation based on RMT as, for the experimental BEC, the low-lying excitations are collective where the interatomic interaction plays a crucial role and the high-lying levels are of a single-particle nature due to the dominating effect of the external harmonic trap.

This paper is organized as follows. Section II deals with the methodology, which includes the many-body technique to calculate the energy levels. The choice of interaction and the correlation function are also discussed in Sec. II. In Sec. III we discuss several statistical tools and results. Section IV concludes and gives a summary.

II. METHODOLOGY

A. Many-body calculation with potential harmonic basis

In order to calculate the energy levels of the condensate we solve the Schrödinger equation with our correlated potential harmonic expansion method (CPHEM) with a short-range correlation function. CPHEM has already been established as a very successful technique for the study of dilute BEC [28–30]. In this method we keep all possible two-body correlations and also use a realistic interatomic interaction, which is clearly an improvement over the mean-field Gross-Pitaevskii (GP) theory [24,31]. We briefly discuss the technique below.

We consider a system of $A = (N + 1)$ identical bosons interacting via two-body potential $V(\vec{r}_{ij}) = V(\vec{r}_i - \vec{r}_j)$ that is confined in an external harmonic potential of frequency ω. The time-independent quantum many-body Schrödinger equation is given by

$$\left[-\frac{\hbar^2}{2m}\sum_{i=1}^{A}\nabla_i^2 + \sum_{i=1}^{A}V_{\rm trap}(\vec{r}_i) + \sum_{i,j>i}^{A}V(\vec{r}_i - \vec{r}_j) - E\right] \times \Psi(\vec{r}_1,\ldots,\vec{r}_A) = 0, \quad (1)$$

where m is the mass of the each boson and E is the energy of the condensate. After eliminating the center of mass motion by using the standard Jacobi vectors [32–34], defined by

$$\vec{\zeta}_i = \sqrt{\frac{2i}{i+1}}\left(\vec{r}_{i+1} - \frac{1}{i}\sum_{j=1}^{i}\vec{r}_j\right) \quad (i = 1,\ldots,N), \quad (2)$$

we obtain the relative motion of the N-body system as

$$\left[-\frac{\hbar^2}{m}\sum_{i=1}^{N}\nabla_{\zeta_i}^2 + V_{\rm trap} + V_{\rm int}(\vec{\zeta}_1,\ldots,\vec{\zeta}_N) - E_R\right] \times \Psi(\vec{\zeta}_1,\ldots,\vec{\zeta}_N) = 0, \quad (3)$$

where $V_{\rm trap}$ is the effective external trapping potential, $V_{\rm int}$ is the sum of all pairwise interactions expressed in terms of the Jacobi vectors, and E_R is the relative energy of the system, i.e., $E = E_R + \frac{3}{2}\hbar\omega$.

Now it should be noted that the hyperspherical harmonic expansion method (HHEM) is an *ab initio* tool to solve the many-body Schrödinger equation where the total wave function is expanded in the complete set of the hyperspherical basis [32]. Although HHEM is a complete many-body approach and includes all possible correlations, it cannot be applied to a typical BEC containing a few thousand to a few million bosons. Due to the large degeneracy of the hyperspherical harmonics (HH) basis, HHEM is restricted only to three-particle systems [32,35]. Since the typical experimental BEC is designed to be very dilute and the probability of three- and higher-body collisions is negligible, we can safely ignore the effect of three- and higher-body correlations. Therefore only the two-body correlation and pairwise interaction among the bosons are important. This allows us to decompose the total wave function Ψ into a two-body Faddeev component for the interacting (ij) pair as

$$\Psi = \sum_{i,j>i}^{A}\phi_{ij}(\vec{r}_{ij}, r). \quad (4)$$

It is worth noting that ϕ_{ij} is a function of two-body separation $\vec{r}_{ij}$ and the global hyperradius r is given by $r = \sqrt{\sum_{i=1}^{N}\zeta_i^2}$. Thus the effect of a two-body correlation comes through the two-body interaction in the expansion basis. ϕ_{ij} is symmetric under P_{ij} for bosons and satisfies the Faddeev equation:

$$[T + V_{\rm trap} - E_R]\phi_{ij} = -V(\vec{r}_{ij})\sum_{k,l>k}^{A}\phi_{kl}, \quad (5)$$

where $T = -\frac{\hbar^2}{m}\sum_{i=1}^{N}\nabla_{\zeta_i}^2$ is the total kinetic energy. Operating $\sum_{i,j>i}$ on both sides of Eq. (5), we get back the original Schrödinger equation. In this approach, we assume that when the (ij) pair interacts, the rest of the bosons are inert spectators. Thus the total hyperangular momentum quantum number and also the orbital angular momentum of the whole system are contributed by the interacting pair only. Next we expand ϕ_{ij} in the subset of HH necessary for the expansion of $V(\vec{r}_{ij})$:

$$\phi_{ij}(\vec{r}_{ij}, r) = r^{-(\frac{3N-1}{2})}\sum_{K}\mathcal{P}_{2K+l}^{lm}\left(\Omega_N^{ij}\right)u_K^l(r). \quad (6)$$

Ω_N^{ij} denotes the full set of hyperangles in the $3N$-dimensional space corresponding to the (ij)th interacting pair, and

$\mathcal{P}^{lm}_{2K+l}(\Omega^{ij}_N)$ is called the potential harmonic (PH) basis. It has an analytic expression:

$$\mathcal{P}^{l,m}_{2K+l}\left(\Omega^{(ij)}_N\right) = Y_{lm}(\omega_{ij})\,{}^{(N)}P^{l,0}_{2K+l}(\phi)\mathcal{Y}_0(D-3); \quad D = 3N, \tag{7}$$

where $\mathcal{Y}_0(D-3)$ is the HH of order zero in the $(3N-3)$-dimensional space spanned by $\{\vec{\zeta}_1, \ldots, \vec{\zeta}_{N-1}\}$ Jacobi vectors and ϕ is the hyperangle given by $r_{ij} = r\cos\phi$. For the remaining $N-1$ noninteracting bosons we define the hyperradius as

$$\rho_{ij} = \sqrt{\sum_{K=1}^{N-1}\zeta_K^2} = r\sin\phi, \tag{8}$$

such that $r^2 = r_{ij}^2 + \rho_{ij}^2$ and r represents the global hyperradius of the condensate. The set of $3N-1$ quantum numbers of HH is now reduced to *only* 3 as for the $N-1$ noninteracting pair:

$$l_1 = l_2 = \cdots = l_{N-1} = 0, \tag{9}$$

$$m_1 = m_2 = \cdots = m_{N-1} = 0, \tag{10}$$

$$n_2 = n_3 = \cdots = n_{N-1} = 0, \tag{11}$$

and for the interacting pair $l_N = l$, $m_N = m$, and $n_N = K$. Thus the $3N$-dimensional Schrödinger equation reduces effectively to a four-dimensional equation with the relevant set of quantum numbers: hyperradius r, orbital angular momentum quantum number l, azimuthal quantum number m, and grand orbital quantum number $2K + l$ for any N. Substituting Eq. (6) into Eq. (5) and projecting on a particular PH, a set of coupled differential equations (CDEs) for the partial wave $u^l_K(r)$ is obtained:

$$\left[-\frac{\hbar^2}{m}\frac{d^2}{dr^2} + V_{\rm trap}(r) + \frac{\hbar^2}{mr^2}\{\mathcal{L}(\mathcal{L}+1) + 4K(K+\alpha+\beta+1)\} - E_R\right]U_{Kl}(r) + \sum_{K'} f_{Kl}V_{KK'}(r)f_{K'l}U_{K'l}(r) = 0, \tag{12}$$

where $\mathcal{L} = l + \frac{3A-6}{2}$, $U_{Kl} = f_{Kl}u^l_K(r)$, $\alpha = \frac{3A-8}{2}$, and $\beta = l + 1/2$; f_{Kl} is a constant and represents the overlap of the PH for the interacting partition with the sum of PHs corresponding to all partitions [34]. The potential matrix element $V_{KK'}(r)$ is given by

$$V_{KK'}(r) = \int P^{lm^*}_{2K+l}\left(\Omega^{ij}_N\right)V(r_{ij})P^{lm}_{2K'+1}\left(\Omega^{ij}_N\right)d\Omega^{ij}_N. \tag{13}$$

B. Choice of interaction and introduction of additional short-range correlations

In the mean-field GP equation the two-body interaction is taken as the contact δ potential, with the interaction strength being proportional to the s-wave scattering length a_s. A positive value of a_s gives a repulsive condensate, and a negative value of a_s gives an attractive condensate. But the contact interaction completely disregards the detailed structure. However, a realistic interatomic interaction, such as the van der Waals potential, is always associated with an attractive $-\frac{C_6}{r_{ij}^6}$ tail at large separation and a strong repulsion at short separation. Depending on the nature of these two parts, a_s can be either positive or negative. In our earlier calculations [36] we have already observed the effect of shape-dependent interatomic interaction in the many-body calculation. So for our present calculation we choose the van der Waals potential with a hard core repulsion of radius r_c, viz., $V(r_{ij}) = \infty$ for $r_{ij} \leqslant r_c$ and $-\frac{C_6}{r_{ij}^6}$ for $r_{ij} > r_c$. The value of C_6 is fixed for a given system, and for ^{87}Rb atoms $C_6 = 6.4898 \times 10^{-11}$ oscillator units (o.u.) [31]. Throughout our calculations we choose $a_{ho} = \sqrt{\frac{\hbar}{m\omega}}$ as the unit of length (o.u.), and energy is also expressed in the units of oscillator energy ($\hbar\omega$). For a given two-body interaction a_s can be obtained from the solution of the two-body equation with zero energy:

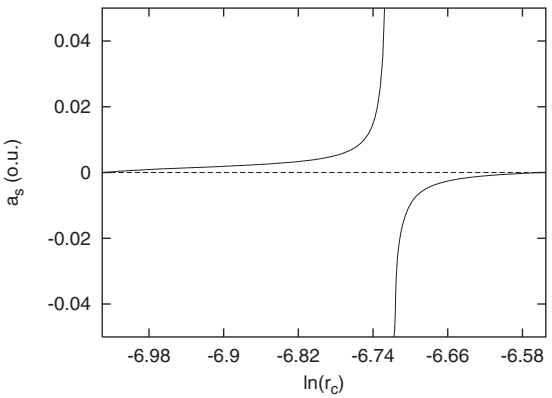

FIG. 1. Plot of scattering length a_s, in oscillator units (o.u.), vs $\ln(r_c)$.

$$-\frac{\hbar^2}{m}\frac{1}{r_{ij}^2}\frac{d}{dr_{ij}}\left(r_{ij}^2\frac{d\eta(r_{ij})}{dr_{ij}}\right) + V(r_{ij})\eta(r_{ij}) = 0. \tag{14}$$

The solution of the two-body equation shows that the value of a_s changes from negative to positive and thus passes through an infinite discontinuity as r_c decreases (Fig. 1). At each discontinuity one extra node appears in the two-body wave function, which corresponds to one extra two-body bound state. With a tiny increase in r_c, across the infinite discontinuity a_s changes drastically from a very large positive value to a large negative value, and the properties of the condensate change drastically [31]. In the GP equation one uses a_s directly without any such detailed knowledge of the actual interatomic potential. For the present calculation we choose $a_s = 0.00433$ o.u., which mimics the Joint Institute for Laboratory Astrophysics (JILA) experiment with ^{87}Rb atoms [9]. The corresponding value of r_c is 1.121×10^{-3} o.u., which causes one node in the two-body wave function. The normalization constant is chosen to make the wave function positive at large r_{ij}.

In the experimental BEC, the Bose gas is extremely dilute, and the average interparticle separation is much larger than the range of the two-body interaction. This is required to prevent the three-body collision and formation of molecules. Thus the pair of particles with practically zero kinetic energy does not come closer than a_s. Although the zeroth-order PH is a constant [33] and will give a large probability even for $r_{ij} \to 0$, it causes very slow convergence in the PH basis

[Eq. (6)]. To compensate for this we additionally include a short-range correlation function $\eta(r_{ij})$ in the PH expansion. As the fundamental assumption in our method is to consider only (ij) pair interaction when the remaining particles are simply inert spectators, the correlation function is obtained as the zero-energy solution of the two-body equation [Eq. (14)]. The correlation function quickly attains an asymptotic form $(1-\frac{a_s}{r_{ij}})$ for large r_{ij}. We replace Eq. (6) by

$$\phi_{ij}(\vec{r}_{ij},r) = r^{-(\frac{3N-1}{2})}\sum_K \mathcal{P}^{lm}_{2K+l}\left(\Omega^{ij}_N\right)u^l_K(r)\eta(r_{ij}). \quad (15)$$

The correlated PH (CPH) basis becomes

$$\left[\mathcal{P}^{l,m}_{2K+l}\left(\Omega^{(ij)}_N\right)\right]_{\text{correlated}} = \mathcal{P}^{l,m}_{2K+l}\left(\Omega^{(ij)}_N\right)\eta(r_{ij}). \quad (16)$$

The correlated potential matrix $V_{KK'}(r)$ is now given by

$$V_{KK'}(r) = \left(h^{\alpha\beta}_K h^{\alpha\beta}_{K'}\right)^{-\frac{1}{2}}\int_{-1}^{+1}\left\{P^{\alpha\beta}_K(z)V\left(r\sqrt{\frac{1+z}{2}}\right)\right.$$
$$\left.\times\, P^{\alpha\beta}_{K'}(z)\eta\left(r\sqrt{\frac{1+z}{2}}\right)W_l(z)\right\}dz. \quad (17)$$

Here $P^{\alpha\beta}_K(z)$ is the Jacobi polynomial, and its norm and weight function are $h^{\alpha\beta}_K$ and $W_l(z)$, respectively [37].

One may note that the inclusion of $\eta(r_{ij})$ makes the PH basis nonorthogonal. One may surely use the standard procedure for handling a nonorthogonal basis. However, in the present calculation we have checked that $\eta(r_{ij})$ differs from a constant value only by small amount and the overlap $\langle\mathcal{P}^{l,m}_{2K+l}(\Omega^{(ij)}_N)|\mathcal{P}^{l,m}_{2K+l}(\Omega^{(kl)}_N)\eta(r_{kl})\rangle$ is quite small. Thus we get back Eq. (12) approximately when the correlated potential matrix is calculated by Eq. (17).

Finally, the CDE, Eq. (12), is solved by the hyperspherical adiabatic approximation (HAA) [38]. In the HAA, one assumes that the hyperradial motion is slow compared to the hyperangular motion. Hence the latter is separated adiabatically and solved for a particular value of r by diagonalizing the potential matrix together with the diagonal hypercentrifugal repulsion in Eq. (12). The lowest eigenvalue, $\omega_0(r)$, is the effective potential for the hyperradial motion, and in this effective potential the entire condensate moves as a single entity. Thus in the HAA, the approximate solution (the energy and wave function) of the condensate is obtained by solving a single uncoupled differential equation:

$$\left[-\frac{\hbar^2}{m}\frac{d^2}{dr^2}+\omega_0(r)-E_R\right]\zeta_0(r)=0, \quad (18)$$

subject to the appropriate boundary conditions on $\zeta_0(r)$. The function $\zeta_0(r)$ is the collective wave function of the condensate in hyperradial space. The lowest-lying state in the effective potential $\omega_0(r)$ corresponds to the ground state of the condensate. The total energy of the condensate is obtained by adding the energy of the center of mass motion $(\frac{3}{2}\hbar\omega)$ to E_R.

Thus by employing the CPHEM and HAA we reduce the multidimensional problem into an effective one-dimensional problem in hyperradial space, and the effective potential $\omega_0(r)$ provides both the qualitative and quantitative descriptions of the system. As in our many-body picture, the collective motion of the condensate is characterized by the effective potential, and the excited states in this potential are the states with nth radial excitation and lth surface mode and are generally denoted by E_{nl}. Thus E_{00} corresponds to the ground state, and $l\neq 0$ corresponds to several surface modes. For $l>0$, we calculate the potential matrix from the diagonal hypercentrifugal term. We have checked that the contribution coming from the off-diagonal matrix element is very small, and we disregard these matrix elements as they make the computation very slow. The calculation of low-lying collective modes is in good agreement with the experimental results and other calculations [39,40]. For energy much larger than the chemical potential μ we observe that the states are separated at an energy close to harmonic oscillator energies $(\sim\hbar\omega)$. This transition from the low-energy collective modes to a high-lying single-particle excitation is further used for the statistical calculations.

III. RESULTS

The integrated level density $N(E)$ has two parts, a smooth part $[\bar{N}(E)]$ and a fluctuating part $[\tilde{N}(E)]$. To compare the fluctuation of different systems or different parts of the same system, the smooth part is removed with the unfolding procedure. Unfolding maps energy levels E_i to ϵ_i with the unit mean level density. For the present analysis the many-body level density is approximated by a polynomial, and unfolding is done with a seven-order polynomial. We unfold each spectrum separately for a specific value of l and form an ensemble having the same symmetry. Then the nearest-neighbor spacing is calculated as $s_i=\epsilon_{i+1}-\epsilon_i$, $i=1,2,\ldots,n$. To study the correlation and level repulsion between energy levels further we utilize the established analogy between the energy spectrum and discrete time series [17–19,41]. The energy spectrum is considered a discrete signal, and the fluctuations of the excitation energy are considered discrete time series. The δ_n statistics has been used in the RMT to study how the consecutive level spacings are correlated. It is defined as

$$\delta_n=\sum_{i=1}^{n}(s_i-\langle s\rangle)=\epsilon_{n+1}-\epsilon_1-n. \quad (19)$$

As the average value of s_i is $\langle s\rangle=1$, and δ_n represents the deviation of $(n+1)$th level from the mean value, i.e., the fluctuation of the $(n+1)$th excited state. It is also closely related to the level density fluctuations, and one can write $\delta_n=-\tilde{N}(E_{n+1})$ if the ground state energy is shifted appropriately [41]. Thus it represents the accumulated level density fluctuation at $E=E_{n+1}$. δ_n is similar to the time series, and n represents the discrete time [18–20,41]. The power spectrum is then defined as the square modulus of the Fourier transform:

$$P^{\delta}_k=\left|\frac{1}{\sqrt{M}}\sum_n\delta_n\exp\left(-\frac{2\pi ikn}{M}\right)\right|^2, \quad (20)$$

where $k=1,2,\ldots,n$, $f=\frac{2\pi k}{M}$ represents the frequency, and M is the size of the series [19]. Therefore, the statistical behavior of the level fluctuation can be established by the $\langle P^{\delta}_k\rangle$ statistic, which measures both short- and long-range correlations. It is verified that the power laws $P^{\delta}_k\propto\frac{1}{k^{\alpha}}$ for both fully chaotic and integrable systems [17–20]. But depending on the level correlation in the chosen system α scales smoothly

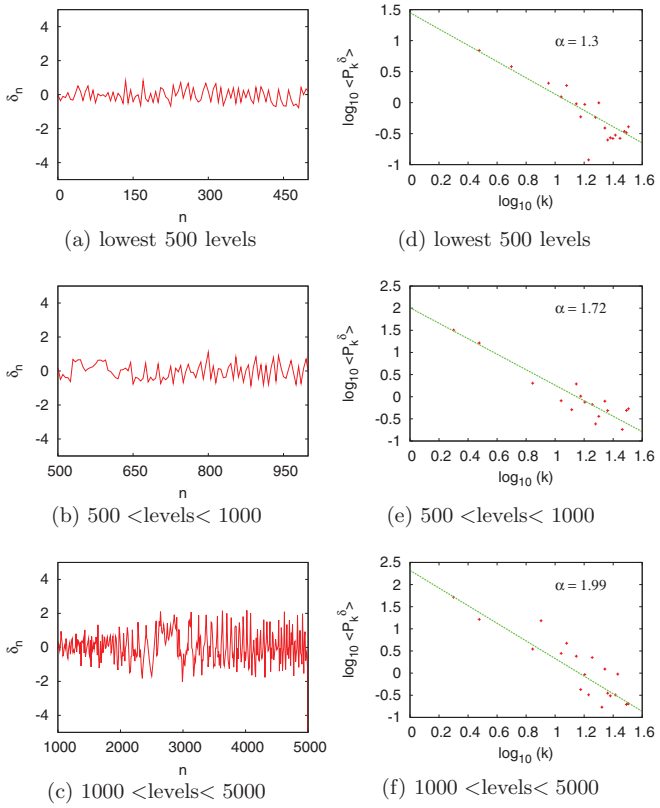

(a) lowest 500 levels (d) lowest 500 levels

(b) 500 <levels< 1000 (e) 500 <levels< 1000

(c) 1000 <levels< 5000 (f) 1000 <levels< 5000

FIG. 2. (Color online) (a)–(c) Fluctuation δ_n statistics for different energy levels n. (d)–(f) Corresponding average power spectra.

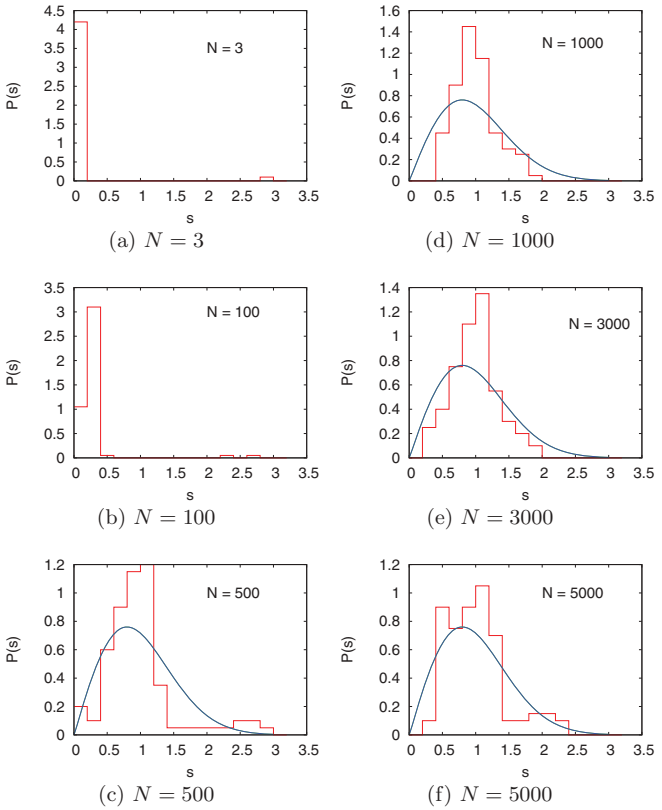

(a) $N = 3$ (d) $N = 1000$

(b) $N = 100$ (e) $N = 3000$

(c) $N = 500$ (f) $N = 5000$

FIG. 3. (Color online) Histogram plot of the $P(s)$ distribution vs s for the lowest 100 levels with different numbers of bosons in the trap. Blue (dark gray) curves present the Wigner distribution.

from 1 (chaotic system) to 2 (for an uncorrelated and integrable system) [17–20]. However, in integrable spin chains of the Halden-Shastry type, the spectral fluctuations exhibit $1/f^4$ noise rather than the expected $1/f^2$ noise [23].

In Fig. 2 we display the energy level fluctuations for different numbers of energy levels for 5000 bosons in the trap. For the low-lying levels we expect level correlation. As the low-lying levels are highly affected by the interatomic interaction, the energy spectra show level repulsion and strong spectral rigidity. This is reflected in Fig. 2(a), which looks like the antipersistent time series for the lowest 500 levels. The δ_n statistics for the low levels is very close to the GOE spectra, which indicates high level correlation due to the interatomic interaction. For the intermediate levels, the effect of the interatomic interaction gradually decreases, and the external trap starts to dominate. Thus the system is expected to show a mixed and complex statistics. When part of the levels are correlated due to interatomic interaction and two-body correlation, the other parts do not repel each other and are uncorrelated. This is similar to the classical mixed system, where part of the phase space is completely regular, with the other part being chaotic. Thus Fig. 2(b) shows that δ_n is neither persistent nor antipersistent. For much higher levels [Fig. 2(c)], the energy levels are uncorrelated due to the dominating effect of the external harmonic trap. The system is close to integrable, and δ_n looks like a persistent series of Poisson spectra. To characterize long-range correlation in Figs. 2(d)–2(f), we plot the average values of the power spectrum $\langle P_k^{\delta} \rangle$ for the same number of levels as reported in Figs. 2(a)–2(c). This shows that the power spectrum follows the scaling law $\langle P_k^{\delta} \rangle \simeq \frac{1}{k^{\alpha}}$. The value of α is presented in Figs. 2(d)–2(f) for different numbers of levels. For low-lying correlated levels $\alpha = 1.31$, for intermediate levels $\alpha = 1.72$, and for high-lying levels $\alpha = 1.99$. Thus α measures not only the chaoticity of the system but also the degree of integrability for complex systems.

At this point we should mention that in an earlier attempt the momentum distribution and temporal power spectra of nonzero temperature Bose-Einstein condensate are calculated using the Gross-Pitaevskii equation [42]. The temporal power spectra also show a $1/f^{\alpha}$ form where $\alpha = 2 - \frac{D}{2}$ (D is the dimension of space) [42,43]. Next to compare the result with the most popular and well known statistics, we calculate the nearest-neighbor spacing distribution $P(s)$ and plot the results in Fig. 3 (and also in Fig. 6). In an earlier attempt in this direction we reported some preliminary results on level spacing distribution $P(s)$ [44]. We have shown that due to interatomic correlation the lower levels are strongly affected by the interaction; however, the higher levels are uncorrelated. But our earlier results do not prove Asaga *et al.*'s statement which says that, in an atomic trap, bosonic atoms are in partly degenerate single-particle states. This makes us very curious to study in detail how the small interatomic interaction will act as a perturbation and lift the degeneracy. This needs further numerical analysis for varying numbers of bosons and with an increase in the number of levels. In Fig. 3 we plot the $P(s)$ distribution for the lowest 100 levels for different numbers of bosons. For $N = 3$ with $a_s = 2.09 \times 10^{-4}$ o.u., the effective

interaction Na_s is 6.27×10^{-4} o.u. The system is very close to integrable as the effect of such small interaction is masked due to the effect of the external harmonic trap. At zero temperature the interaction energy for $N = 3$ is almost negligible compared to the trap energy. Thus the small interaction acts as a very small perturbation, and the exact degeneracy in the external 3D harmonic trap is lifted, which results in the existence of large quasidegenerate states. The $P(s)$ distribution exhibits a δ type peak called the Shnirelman peak. In 1993, Shnirelman showed that for systems with time reversal symmetry should exhibit such a δ-function peak near $s = 0$ in the $P(s)$ distribution. This peak appears due to the presence of symmetry, and separating levels by symmetry, one will get back the Poisson distribution. This indicates the presence of bulk quasidegenerate states in the level spacing distribution. In the first verification of the Shnirelman theorem, Chirikov and Shepelyansky studied the kicked rotator on a torus with time reversal symmetry [45]. Later the theorem was verified in a more real physical quantum system. The Calogero-like three-body problem was studied, where the hidden continuous symmetry was broken by adding a three-body interaction term [46]. With N gradually increasing further in the trap, the lower levels show level repulsion, and the system smoothly changes from close to integrability to nonintegrability. The corresponding $P(s)$ distribution smoothly changes to a Wigner-like distribution with an increase in N. Due to strong interatomic interaction the system becomes more correlated and shows level repulsion.

In our present problem of trapped interacting bosons, the exact degeneracy comes from the external harmonic trap. However due to the weak interatomic interaction, the effect of exact degeneracy is gradually lifted, and it results in the quasidegeneracy when the number of bosons in the trap is quite small. For better resolution of the Shnirelman peak in Fig. 3 (with $N = 3$) we plotted the same peak in Fig. 4 in finer detail. A huge peak in the first bin of the histograms clearly demonstrates the existence of global quasidegeneracy, in accordance with the Shnirelman theorem. In Fig. 4(a), we

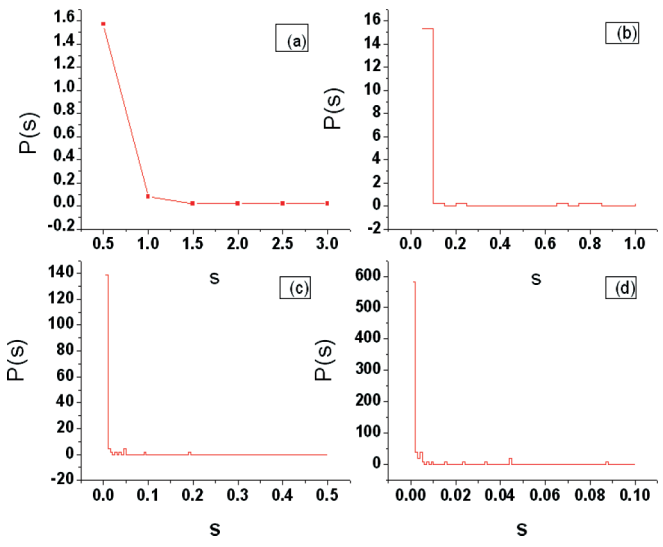

FIG. 4. (Color online) Level spacing distribution $P(s)$ for the lowest 100 levels with three atoms in the trap. The Shnirelman peak is shown in finer detail.

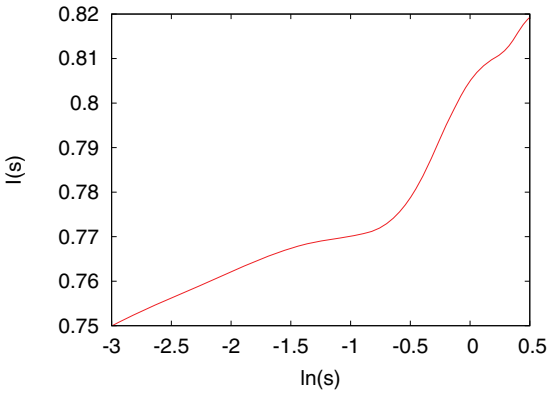

FIG. 5. (Color online) Plot of integral level spacing distribution $I(s)$ vs $\ln(s)$.

observe the peak has a finite width which is further associated with the Poissonian tail. This peak contains important information about the structure of the quantum system. The resolution of the peak is further plotted in Fig. 5, where we present the integral level spacing distribution $I(s) = \int_0^s P(s)$, normalized to unity. It has two separate regions. The rightmost steep increase of $I(s)$ corresponds to the Poissonian tail of Fig. 4. The leftmost part is more interesting. It shows the linear dependence between I and $\ln(s)$, which represents the structure of the Shnirelman peak.

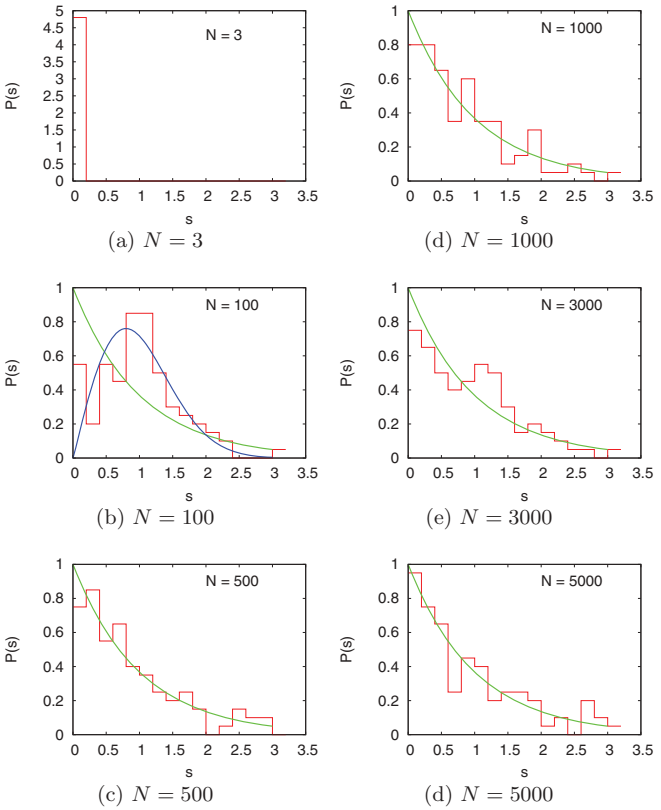

FIG. 6. (Color online) Histogram plot of $P(s)$ distribution vs s for different numbers of bosons N for energy levels 3900 to 4000. Green (light gray) curves correspond to Poisson distribution while the blue (dark gray) curve presents the Wigner distribution.

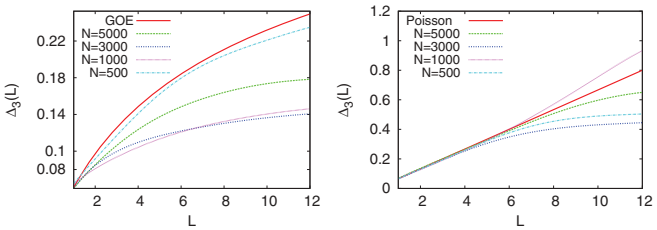

(a) lowest 100 levels (b) 3900 < levels < 4000

FIG. 7. (Color online) Spectral average $\langle\Delta_3(L)\rangle$ computed for the Hamiltonian (1) with different numbers of interacting bosons N in the external trap vs L (a) for the lowest 100 energy levels and (b) for energy levels between 3900 and 4000.

The results for higher levels (close to level 4000) and for the same set of N values as reported in Fig. 3 are plotted in Fig. 6. For $N = 3$, the $P(s)$ distribution again shows the sharp peak as expected. As the high-lying excitations are of a single-particle nature, the energy levels are now uncorrelated, and the corresponding $P(s)$ distribution shows a Poisson type fluctuation with an increase in the number of bosons. It confirms that for higher levels the system again becomes close to integrable as the effect of the external trap strongly dominates. The observation is in agreement with the earlier observation of the δ_n statistics and power spectrum. $P(s)$ measures the short-range correlation. The Δ_3 statistic is usually used to investigate the long-range correlation. It gives the statistical measure of the rigidity of finite spectral level sequence. For a given energy interval L, it is determined by the least squares deviation of the staircase from the best straight line fit. In Fig. 7 we plot the spectral average $\langle\Delta_3(L)\rangle$ for different energy levels. For higher energy levels $\langle\Delta_3(L)\rangle$ bends to Poissonian whereas for low-lying collective levels it is close to the GOE prediction.

IV. CONCLUSIONS

In summary, we have shown that the analogy between quantum energy spectra and time series is an efficient and powerful way to characterize quantum level fluctuation. Although the statistical behavior of level fluctuation and the corresponding power spectrum are understood for fully chaotic and completely integrable systems, the behaviors of the power spectrum in the mixed regime between integrability and chaos is interesting. Interacting trapped bosons are a very complex system, and due to the existence of two energy scales it nicely describes chaos to order transition with an increase in the number of energy levels. Our observation of the Shnirelman peak strongly proves the earlier statement of Asaga *et al*. [11]. Our results nicely demonstrate how the degenerate single-particle states of the pure harmonic trap are lifted gradually by increasing the effective interatomic interaction. Our findings are quite different from the results seen in atomic nuclei, atoms, and molecules [15]. Interacting trapped bosons are a very special and very complex system where the low-lying collective excitations are strongly influenced by interatomic interaction and show level repulsion. It is also spatially inhomogeneous, and the high-lying levels are of a single-particle nature and have regular features. For the dilute interacting Bose gas, it is also possible to calculate a large number of energy levels with high statistical precision. They can also be measured experimentally. The corresponding level fluctuation shows a transition from close to a Wigner distribution to a Poisson distribution with an increase in energy levels, showing it does not follow GOE predictions, and we need a modified GOE which combines uniform, GOE, and Poisson distributions [47]. We observe the existence of the $1/f^{\alpha}$ power law in the energy spectrum. The parameter α measures the fluctuation properties of the quantum system through the power spectrum. As the interacting trapped bosons are interesting in light of recent experiments on BEC, our system is generic, and it confirms that $1/f^{\alpha}$ noise is ubiquitous in nature. However, some open questions still remain, namely, how the spectral distribution will change with attractive interactions so that we can study the dynamical behavior of the energy spectrum.

ACKNOWLEDGMENTS

We thank Prof Luca Salasnich for some fruitful discussions. This work is supported by the Department of Atomic Energy (DAE), government of India, through Grant No. 2009/37/23/BRNS/1903. A.B. acknowledges the Council of Scientific and Industrial Research (CSIR), India, for a senior research fellowship [Grant No. 09/028(0773)-2010-EMR-1]. S.K.H. also acknowledges CSIR, India, for a junior research fellowship [Grant No. 08/561(0001)/2010-EMR-1].

[1] O. Bohigas, M. J. Giannoni, and C. Schmit, Phys. Rev. Lett. **52**, 1 (1984).
[2] H.-J. Stöckmann, *Quantum Chaos* (Cambridge University Press, Cambridge, 1999).
[3] T. A. Brody, J. Flores, J. B. French, P. A. Mello, A. Pandey, and S. S. M. Wong, Rev. Mod. Phys. **53**, 385 (1981).
[4] V. K. B. Kota, Phys. Rep. **347**, 223 (2001).
[5] J. M. G. Gómez, K. Kar, V. K. B. Kota, R. A. Molina, A. Relaño, and J. Retamosa, Phys. Rep. **499**, 103 (2011).
[6] N. D. Chavda, V. Potbhare, and V. K. B. Kota, Phys. Lett. A **311**, 331 (2003).
[7] J. L. Roberts, N. R. Claussen, S. L. Cornish, E. A. Donley, E. A. Cornell, and C. E. Wieman, Phys. Rev. Lett. **86**, 4211 (2001); J. L. Roberts, N. R. Claussen, J. P. Burke, C. H. Greene, E. A. Cornell, and C. E. Wieman, *ibid*. **81**, 5109 (1998).
[8] K. B. Davis, M. O. Mewes, M. R. Andrews, N. J. van Druten, D. S. Durfee, D. M. Kurn, and W. Ketterle, Phys. Rev. Lett. **75**, 3969 (1995).
[9] M. H. Anderson, J. R. Ensher, M. R. Matthews, C. E. Wieman, and E. A. Cornell, Science **269**, 198 (1995).
[10] S. L. Cornish, N. R. Claussen, J. L. Roberts, E. A. Cornell, and C. E. Wieman, Phys. Rev. Lett. **85**, 1795 (2000).
[11] T. Asaga, L. Benet, T. Rupp, and H. A. Weidenmüller, Ann. Phys. (N.Y.) **298**, 229 (2002).
[12] W. Hai, Q. Zhu, and S. Rong, Phys. Rev. A **79**, 023603 (2009).

[13] D. Poletti, L. Fu, J. Liu, and B. Li, Phys. Rev. E **73**, 056203 (2006).
[14] J. Cheng, Phys. Rev. A **81**, 023619 (2010).
[15] O. Bohigas, *Random Matrix Theories and Chaotic Dynamics*, Les Houches, Session LII, (1989), Chaos and Quantum Physics, Course 2, edited by M.-J. Giannoni, A. Voros and J. Zinn-justin (Elsevier Science Publishers B.V., North Holland, 1991).
[16] A. Yamamoto, S. Yamada, M. Okumura, and M. Machida, Phys. Rev. A **84**, 043642 (2011).
[17] A. Relano, J. M. G. Gomez, R. A. Molina, J. Retamosa, and E. Faleiro, Phys. Rev. Lett. **89**, 244102 (2002).
[18] A. Relano, J. Retamosa, E. Faleiro, R. A. Molina, and A. P. Zuker, Phys. Rev. E **73**, 026204 (2006).
[19] J. M. G. Gomez, A. Relano, J. Retamosa, E. Faleiro, L. Salasnich, M. Vranicar, and M. Robnik, Phys. Rev. Lett. **94**, 084101 (2005).
[20] A. Relano, Phys. Rev. Lett. **100**, 224101 (2008).
[21] M. S. Santhanam and J. N. Bandyopadhyay, Phys. Rev. Lett. **95**, 114101 (2005).
[22] M. Fliesser and R. Graham, Phys. D **131**, 141 (1999).
[23] J. C. Barba, F. Finkel, A. González-López, and M. A. Rodríguez, Phys. Rev. E **80**, 047201 (2009).
[24] F. Dalfovo, S. Giorgini, L. P. Pitaevskii, and S. Stringari, Rev. Mod. Phys. **71**, 463 (1999).
[25] D. S. Jin, J. R. Ensher, M. R. Matthews, C. E. Wieman, and E. A. Cornell, Phys. Rev. Lett. **77**, 420 (1996).
[26] F. Dalfovo, S. Giorgini, M. Guilleumas, L. Pitaevskii, and S. Stringari, Phys. Rev. A **56**, 3840 (1997).
[27] M.-C. Chung and A. B. Bhattacharjee, New J. Phys. **11**, 123012 (2009).
[28] T. K. Das and B. Chakrabarti, Phys. Rev. A **70**, 063601 (2004).
[29] T. K. Das, S. Canuto, A. Kundu, and B. Chakrabarti, Phys. Rev. A **75**, 042705 (2007).
[30] T. K. Das, A. Kundu, S. Canuto, and B. Chakrabarti, Phys. Lett. A **373**, 258 (2009).
[31] C. J. Pethick and H. Smith, *Bose-Einstein Condensation in Dilute Gases* (Cambridge University Press, Cambridge, 2001).
[32] J. L. Ballot and M. Fabre de la Ripelle, Ann. Phys. (NY) **127**, 62 (1980).
[33] M. Fabre de la Ripelle, Ann. Phys. (NY) **147**, 281 (1983).
[34] M. Fabre de la Ripelle, Few Body Syst. **1**, 181 (1986).
[35] B. D. Esry and C. H. Greene, Phys. Rev. A **60**, 1451 (1999).
[36] B. Chakrabarti and T. K. Das, Phys. Rev. A **78**, 063608 (2008).
[37] M. Abramowitz and I. A. Stegun, *Handbook of Mathematical Functions* (Dover, New York, 1972), p. 773.
[38] T. K. Das, H. T. Coelho, and M. Fabre de la Ripelle, Phys. Rev. C **26**, 2281 (1982).
[39] P. K. Debnath and B. Chakrabarti, Phys. Rev. A **82**, 043614 (2010).
[40] A. Biswas and T. K. Das, J. Phys. B **41**, 231001 (2008).
[41] E. Faleiro, J. M. G. Gómez, R. A. Molina, L. Muñoz, A. Relano, and J. Retamosa, Phys. Rev. Lett. **93**, 244101 (2004).
[42] K. Staliunas, Int. J. Bifurcation Chaos **16**, 2713 (2006).
[43] K. Staliunas, Int. J. Bifurcation Chaos **11**, 2845 (2001).
[44] B. Chakrabarti, A. Biswas, V. K. B. Kota, K. Roy, and S. K. Haldar, arxiv:1101.5469 [cond-mat.quant-gas].
[45] B. V. Chirikov and D. L. Shepelyansky, Phys. Rev. Lett. **74**, 518 (1995).
[46] B. Chakrabarti and B. Hu, Phys. Rev. E **65**, 067103 (2002).
[47] T. A. Guhr and H. A. Weidenmüller, Ann. Phys. (NY) **193**, 472 (1989).